Polyacrylamide–Clay Nanocomposite Materials Prepared by Photopolymerization with Acrylamide as an Intercalating Agent

Jui-Ming Yeh, Shir-Joe Liou, Ya-Wen Chang

Department of Chemistry and Center for Nanotechnology, Chung-Yuan Christian University, Chung Li, Taiwan 320, Republic of China

Received 22 January 2003; accepted 19 August 2003

ABSTRACT: A series of nanocomposite materials consisting of water-soluble polyacrylamide (PAA) and layered montmorillonite (MMT) clay platelets were prepared by the effective dispersion of the inorganic nanolayers of the MMT clay in the organic PAA matrix via *in situ* ultraviolet-radiation polymerization. The acrylamide monomers functioned as both the intercalating agent and the reacting monomers. As a representative procedure for the preparation of the nanocomposites, organic acrylamide monomers were first intercalated into the interlayer regions of acrylamide-treated organophilic clay hosts, and this was followed by one-step ultraviolet-radiation free-radical polymerization with benzil as a photoinitiator. The as-prepared polyacrylamide–clay nanocomposite (PCN) materials were subsequently characterized by Fourier transform infrared spectroscopy, wide-angle powder X-ray diffraction, and transmission electron microscopy. The effects of the material composition on the thermal stability, optical clarity, and gas-barrier properties of pristine PAA and PCN materials, in the forms of fine powders and membranes, were also studied by differential scanning calorimetry, thermogravimetric analysis, ultraviolet–visible transmission spectroscopy, and gas permeability analysis. The molecular weights of PAA extracted from PCN materials and pristine PAA were determined by gel permeation chromatography with tetrahydrofuran as an eluant. J Appl Polym Sci 91: 3489–3496, 2004

Key words: nanocomposites; photopolymerization; clay

INTRODUCTION

Montmorillonite (MMT) is a clay mineral consisting of stacked silicate sheets approximately 10 Å thick and approximately 2180 Å long.[1] It possesses a high aspect ratio and demonstrates a plate morphology. The chemical structure of MMT consists of two fused silica tetrahedral sheets sandwiching an edge-shared octahedral sheet of either magnesium or aluminum hydroxide. Na^+ and Ca^{+2} existing in the interlayer regions can be replaced with organic cations, such as alkyl ammonium ions, by a cation-exchange reaction to make the silicate hydrophilic layer organophilic. Because lamellar structures have a high in-plane strength, stiffness, and aspect ratio, layered materials such as smectite clays (e.g., MMT) have evoked intense and extensive research interest lately for the preparation of various novel polymer–clay nanocomposite materials with advanced gas-barrier properties,[2] thermal stability,[3] mechanical strength,[4] fire retardance,[5] and corrosion protection.[6] Several research groups have devoted their efforts to the study of nanocomposites of polyacrylamide (PAA) and clay in a gel form. For example, Gao et al.[7] reported the rheological properties of PAA–bentonite composite hydrogels. Churochkina et al.[8] studied the swelling and collapse of gel composites of PAA gels containing MMT.

In this study, we prepared a series of polyacrylamide–clay nanocomposite (PCN) materials by an *in situ* ultraviolet (UV)-radiation polymerization process. Subsequently, as-prepared PCN materials were characterized by Fourier transform infrared (FTIR) spectroscopy, wide-angle powder X-ray diffraction, and transmission electron microscopy (TEM). The effects of the material composition on the thermal stability, optical clarity, and gas-barrier properties of PAA and PCN materials, in the form of fine powders and membranes, were also studied by differential scanning calorimetry (DSC), thermogravimetric analysis (TGA), ultraviolet–visible (UV–vis) transmission spectroscopy, and gas permeability analysis (GPA), respectively. The molecular weights of PAA extracted from PCN materials and bulk PAA were determined by gel permeation chromatography (GPC) with tetrahydrofuran (THF) as an eluant.

EXPERIMENTAL

Chemicals and instrumentation

Acrylamide (99%; Sigma) was used as an intercalating agent and reacting monomer, and benzil (99%; Sigma,

Correspondence to: J.-M. Yeh (juiming@cycu.edu.tw).
Contract grant sponsor: National Science Council; contract grant number: 92-2113-M-033-011.

Journal of Applied Polymer Science, Vol. 91, 3489–3496 (2004)

Switzerland) was used as a free-radical photoinitiator. Both were used as received without further purification. MMT (PK 805) was supplied by Pai-Kong Ceramic Co. (Taiwan). The light source was a 100-W Blak-Ray photochemical reactor lamp (Upland, USA); the long wavelength (365 nm) was 15 cm between the lamp and the surface of the reaction mixture.

A wide-angle X-ray diffraction study of the samples was performed on a Rigaku D/MAX-3C OD-2988N X-ray diffractometer (Japan) with a cooper target and a nickel filter at a scanning rate of 4°/min. The samples for a TEM study were prepared by the placement of the powder of PCN materials into epoxy resin capsules and the curing of the epoxy resin at 100°C for 24 h in a vacuum oven. Then, the cured epoxy resin containing PCN materials was microtomed with a Reichert-Jung Ultracut-E (Japan) into 60–90-nm-thick slices. Subsequently, one layer of carbon about 10 nm thick was deposited on these slices on 100-mesh copper nets for TEM observations on a JEOL 200FX (Peabody, MA) with an acceleration voltage of 120 kV.

A PerkinElmer thermal analysis system equipped with a model 7 DSC instrument and a model 7/DX TGA instrument was used for the thermal analyses under an air flow. The programmed heating rate was 20°C/min. FTIR spectra were recorded on pressed KBr pellets with a Bio-Rad FTS-7 FTIR spectrometer (Bio-Rad, Hercules, CA). A gas permeability analyzer (model GTR 10, Yanagimoto Co., Ltd.) was used to perform the permeation experiment for oxygen and nitrogen gas. The UV–vis transmission spectra of polymeric membranes in N-methyl-2-pyrrolidone were recorded on a Hitachi U-2000 UV–vis spectrometer at room temperature. The molecular weights of the polymers extracted from all composite samples and bulk PAA was determined on a Waters model 2 II GPC instrument equipped with a model 590 programmable solvent delivery module (Medford, MA), a differential refractometer detector, and a Styragel HT column with THF as an eluant and monodispersed polystyrenes as calibration standards.

Photopolymerization of PAA

In a typical procedure, 10 g (0.3 mol) of acrylamide was dissolved in 200 mL of methanol under vigorous magnetically stirring for 1 h. Benzil (6.8 g, 0.06 mol) was added slowly. The reaction mixture was stirred magnetically and irradiated with a UV light housed in a light-proof box for 24 h. The light source was a 100-W Blak-Ray photochemical reactor lamp; the long wavelength (365 nm) was 15 cm between the lamp and the surface of the reaction mixture. The raw product was obtained by suction and drying *in vacuo* at room temperature for 24 h.

Preparation of organophilic clay

Organophilic clay was prepared by a typical cation-exchange reaction between the sodium cations of MMT clay and the alkyl ammonium ions of the intercalating agent, acrylamide. Typically, 5 g of MMT clay (PK805) was stirred in 600 mL of distilled water (beaker A) at room temperature overnight. A separate solution contained 0.42 g of acrylamide in another 30 mL of distilled water (beaker B) with magnetic stirring; this was followed by the addition a 1.0*M* HCl aqueous solution to adjust the pH value to about 3–4. After 1 h of stirring, the protonated amino acid solution (beaker B) was added at a rate of approximately 10 mL/min with vigorous stirring to the MMT suspension (beaker A). The mixture was stirred overnight at room temperature. The organophilic clay was recovered by ultracentrifugation (9000 rpm, 30 min) and filtration of the solution in a Buchner funnel. The purification of the products was performed by the repeated washing and filtration of the samples (at least three times) for the removal of any excess of ammonium ions.

Photochemical preparation of PCN materials

A typical procedure for the preparation of a PCN material with a 1 wt % clay loading was as follows. First, 0.1 g of the organophilic clay was added to 200 mL of methanol under magnetic stirring overnight at room temperature. The acrylamide monomer (10 g, 0.3 mol) and benzil (24.3 g, 0.15 mol) were subsequently added to the solution, which was stirred for another 24 h at room temperature. The reaction mixture was subsequently stirring and irradiated with a UV light housed in a light-proof box for 24 h. As-prepared precipitates were then obtained by filtration and drying in a vacuum oven at room temperature for 24 h.

Polymer recovery (extraction)

A reverse cation-exchange reaction was used to separate bound PAA from the inorganic component in the nanocomposites.[9] In a typical extraction procedure, 2 g of a fine powder of as-prepared PCN was dissolved in approximately 100 mL of THF (beaker A). Separately, a 10-mL stock solution of 1 wt % lithium chloride in THF was prepared (beaker B). Both beakers were vigorously magnetically stirred for 3–4 h at room temperature. After the contents of the two beakers were combined, the mixture was stirred overnight, and this was followed by Soxhlet extraction at 80°C for 24 h. The extract solution was then poured into an excess amount of *n*-hexane to precipitate the polymer. After filtration, the polymer was dried *in vacuo* at room temperature for 48 h. The molecular

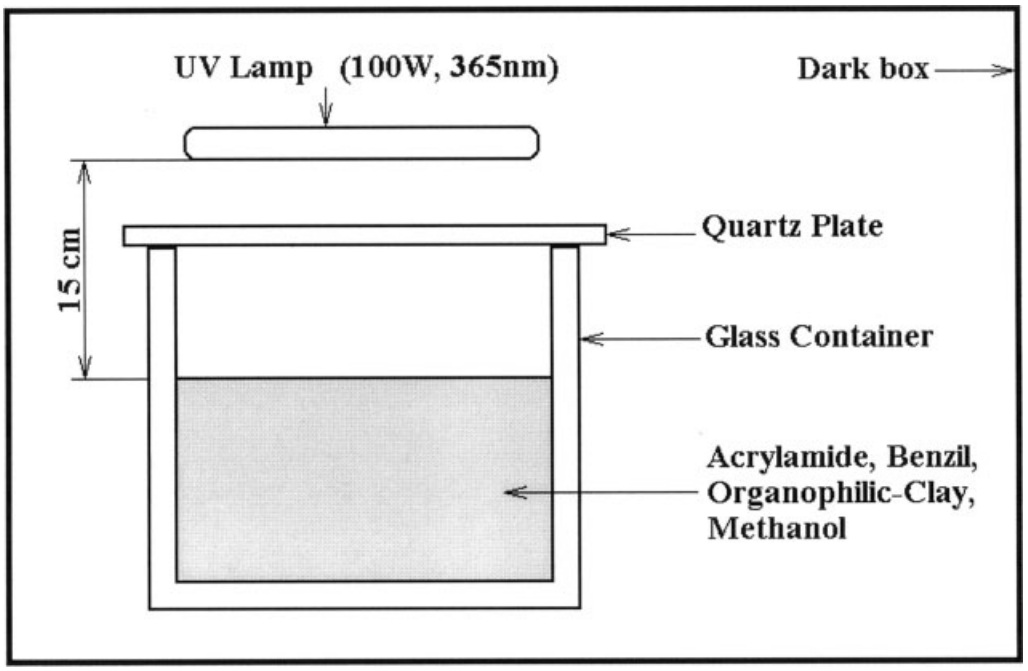

Figure 1 Experimental setup of photopolymerization for the preparation of the PCN materials.

weights of both extracted and bulk PAA were determined by GPC analyses with THF as an eluant.

RESULTS AND DISCUSSIONS

For the preparation of the PCN materials, the acrylamide monomers were first intercalated into the interlayer region of organophilic clay, and this was followed by *in situ* photochemical polymerization in the presence of the photoinitiator under UV radiation. The reaction system was housed in a light-proof box, as illustrated in Figure 1. The composition of the PCN materials was varied from 0 to 10 wt % clay with respect to the PAA content.

Characterization

The characteristic FTIR spectra of the organophilic clay, bulk PAA, and PCN materials, are given in Figure 2. The representative vibration bands of PAA are at 1630–1680 (C═O) and 3190 and 3350 cm^{-1} (—NH_2); those of the MMT clay appear at 1040 (Si—O), 600 (Al—O), and 420 cm^{-1} (Mg—O).[6] As the loading of the MMT clay is increased, the intensities of the MMT clay bands become stronger in the FTIR spectra of the PCN materials. Figure 3 shows the wide-angle powder X-ray diffraction patterns of the organophilic clay and a series of PCN materials. There is a lack of any diffraction peak of CLAA1, i.e., 1 wt % loading of clay in polyacrylamide matrix, at 2θ = 2–10°, as opposed to the diffraction peak at 2θ = 6.7° (*d*-spacing = 13.2 nm) for the organophilic clay; this indicates the possibility of having exfoliated silicate nanolayers of the organophilic clay dispersed in the PAA matrix. The X-ray diffraction scanning rate is given as 4° (θ)/min. The X-ray diffraction data at a lower scanning rate (e.g., 1°/min) show a similar situation. As the clay loading increases to 3 wt %, CLAA3 exhibits a diffraction peak at 2θ = 4.3° (*d*-spacing = 20.5 nm). This implies that there is a small amount of the organophilic clay that cannot be exfoliated in PAA and that exists in the form of an intercalated layer structure. When the clay loading increases up to 10 wt % (CLAA10), the interlayer distance of the organoclay nanolayers cannot be further increased, and there is a *d*-spacing of the organophilic clay in the organic PAA matrix, indicating that a large amount of the organoclay exists in an intercalated layer structure.

Transmission electron micrographs of PCN material incorporation with 5 wt % clay show that the nanocomposites have a mixed nanomorphology. Exfoliated silicate layers and larger intercalated tactoids can both be found in the PAA matrix, as shown in Figure 4(a) at 50,000×. A lower magnification image, displayed in Figure 4(b) at 10,000×, showing global clay dispersion, exhibits the majority of the intercalated clay plates present.

Weight-average molecular weight determination of extracted and bulk PAA

The molecular weights of the various polymer samples recovered from the nanolayers of MMT clays

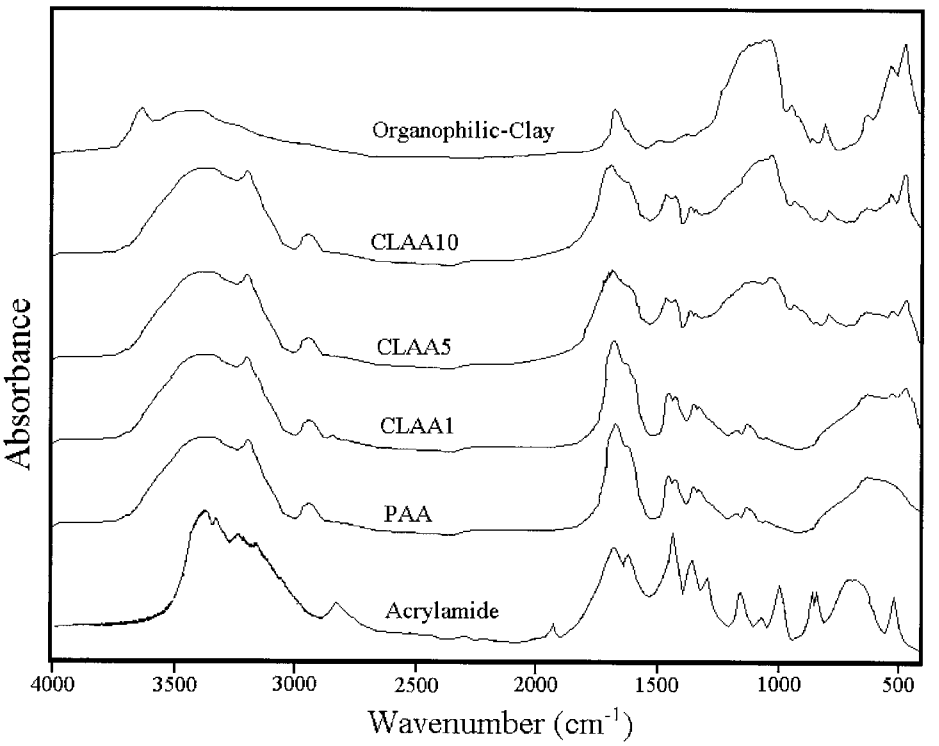

Figure 2 FTIR spectra of the organophilic clay, PAA, and a series of PCN materials.

were obtained by GPC analyses with THF as an eluant. All the GPC elution patterns of the samples display a single peak, corresponding to a molecular weight value, as shown in Table I. The molecular weights of extracted PAA are significantly lower than that of bulk PAA, and this indicates the structurally

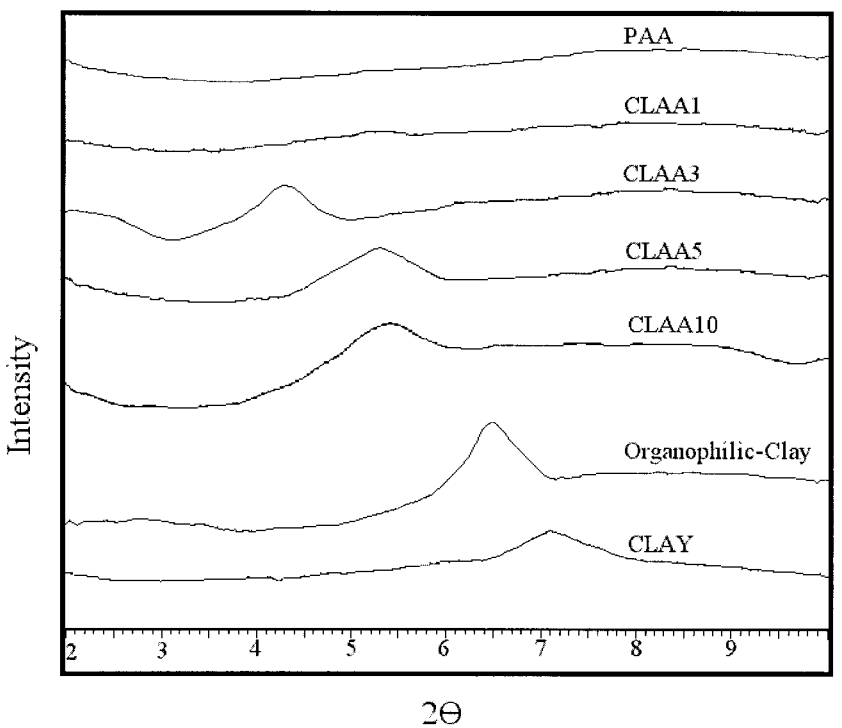

Figure 3 Wide-angle powder X-ray diffraction patterns of the organophilic clay, PAA and a series of PCN materials.

restricted polymerization situations in the intragallery region of the MMT clay[6,10] or the nature of the clay–oligomer interactions, such as adsorption, during the polymerization reaction.

Thermal properties of fine powders

Figure 5 shows typical TGA curves of the PCN materials and PAA, as measured under an air atmosphere. In general, there appear to be several stages of weight loss, which start at approximately 200°C and end at 800°C and which may correspond to the degradation of the intercalating agent followed by the structural decomposition of the polymers. According to the published reports on polymer–clay nanocomposite materials, the unparalleled ability of smectite clays boosts the thermal stability of polymers.[3] Evidently, the onset of the thermal decomposition of the nanocomposites shifts significantly toward a temperature range higher than that of pristine PAA, and this confirms the enhancement of the thermal stability of the intercalated polymer.[6b,c] After approximately 600°C, the curves all become flat, and mainly the inorganic residues (i.e., Al_2O_3, MgO, and SiO_2) remain. From the amounts of the residues at 600°C, the inorganic contents in the original PCN materials were obtained, and they were significantly higher than the values calculated from the feed composition. The calculated inorganic contents tend to be lower than those determined from TGA. This situation was reported by other research groups as well.[11,12] We also find from DSC measurements (Fig. 6) that the incorporation of the MMT clay into PAA results in an increase in the glass-transition temperature (heating scan) with respect to pristine PAA. This is tentatively attributed to the confinement of the intercalated polymer chains within the clay galleries, which prevent the segmental motions of the polymer chains.[6] As the loading of the MMT clay is increased, the glass-transition temperature of the PCN materials becomes higher.

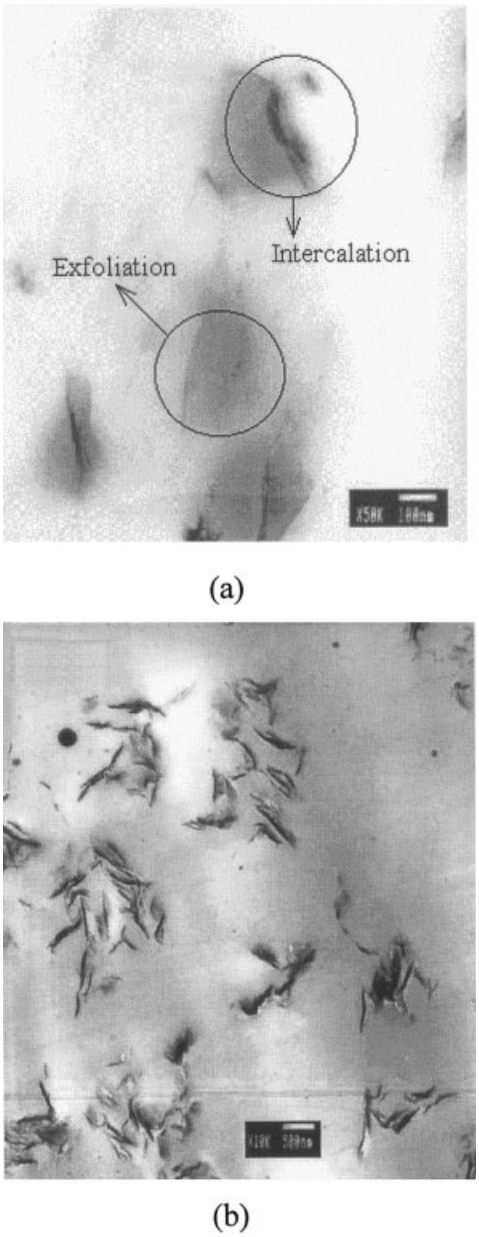

Figure 4 TEM images of CLAA5, showing exfoliated single, double, and triple layers and a multilayer tactoid: (a) 50,000× and (b) 10,000×.

TABLE I
Molecular Weights of Bulk and Extracted PAAs

Sample	M_w	M_n	M_w/M_n
PAA	41,200	8,400	4.90
CLAA1	27,200	10,300	2.64
CLAA3	21,100	8,300	2.54
CLAA5	18,900	7,500	2.52
CLAA10	14,600	5,900	2.47

M_w = weight-average molecular weight; M_n = number-average molecular weight.

Optical clarity and gas-barrier properties of membranes

Because of the nanoscale dispersion of the clays in the PAA matrix, optical clarity remains high at low clay contents (e.g., CLAA1), which yield primarily exfoliated composites.[6,13,14] Figure 7 shows the UV–vis transmission spectra of pure PAA and PCN materials incorporating various clay loadings. These membranes are approximately 80 ± 1 μm thick. The spectra of CLAA1 show that the visible region (400–700 nm) is slightly affected by the presence of the 1 wt % clay loading and retains the high transparency of PAA. For example, a decrease of about 10% in the UV–vis transmission was observed for a CLAA membrane at 400 nm. However, the spectra of PCN materials with in-

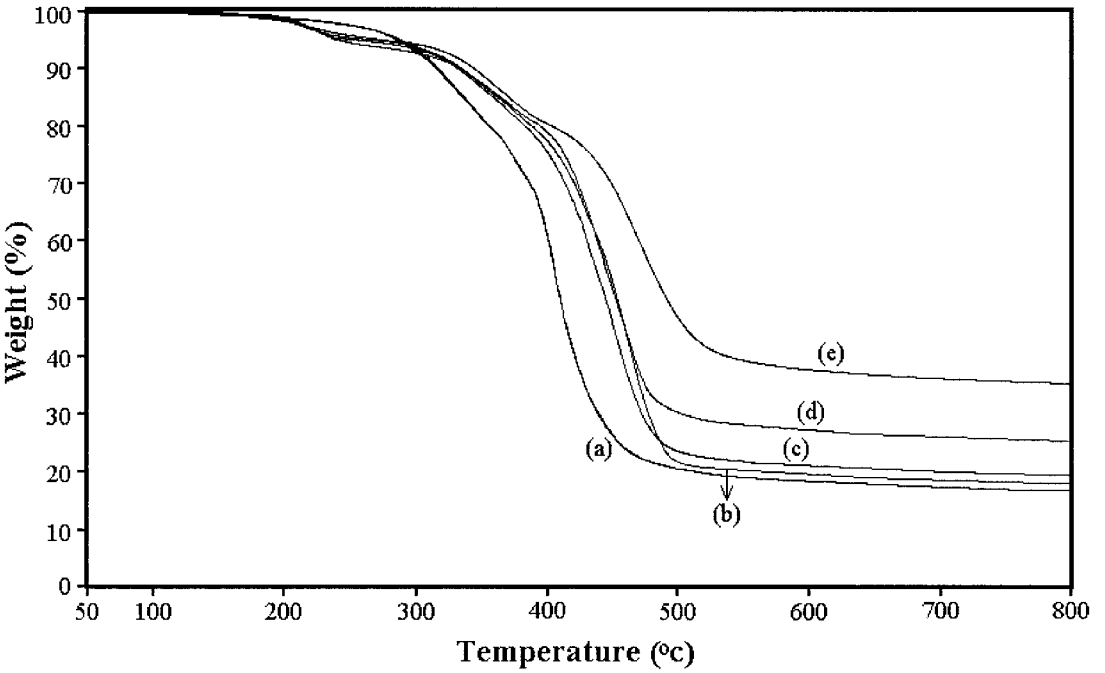

Figure 5 TGA curves of (a) PAA, (b) CLAA1, (c) CLAA3, (d) CLAA5, and (e) CLAA10.

creasing higher clay loadings (e.g., CLAA3, CLAA5, and CLAA10) exhibit a lower transparency of PAA, reflecting the primarily intercalated composites. For the UV wavelength, there is strong scattering or absorption, and this results in a very low transmission of UV light.

From a molecular barrier study, we find that the dispersion of clay platelets into the PAA matrix promotes the molecular barrier of O_2 and N_2 gas. Moreover, a further increase in the clay loading results in a further enhanced molecular barrier property of the PCN materials,[6] as illustrated in Figure 8.

CONCLUSIONS

In this study, a series of nanocomposite materials consisting of water-soluble PAA and layered MMT clay platelets were prepared by the effective dispersion of

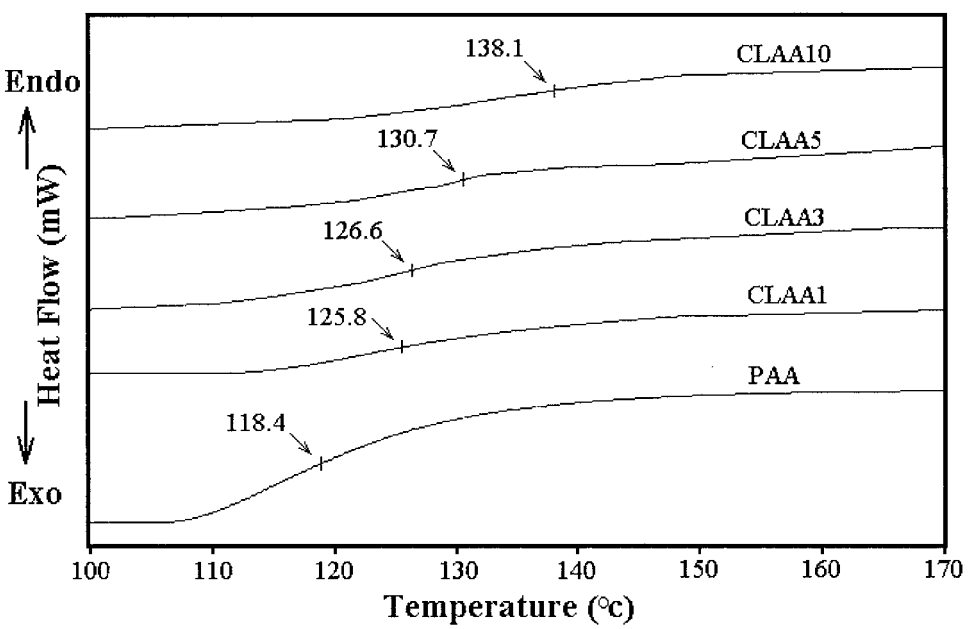

Figure 6 DSC curves of PAA and a series of PCN materials.

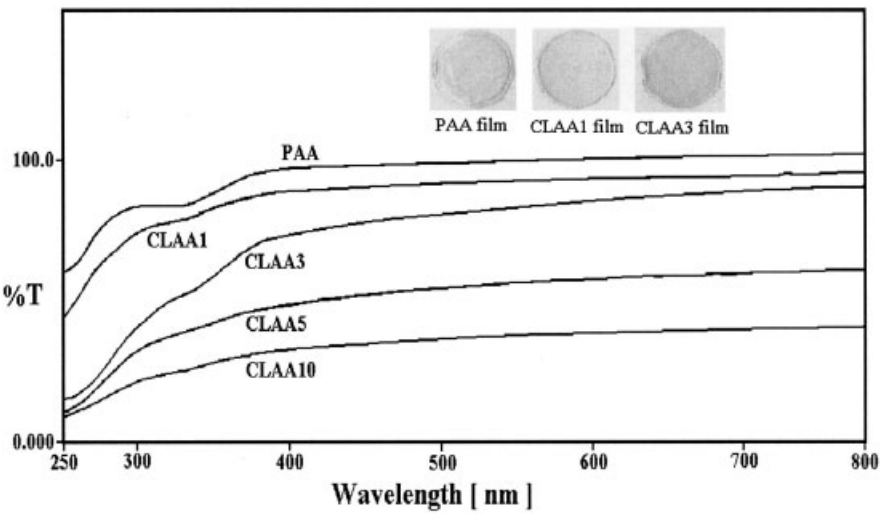

Figure 7 UV–vis transmission spectra of PAA and a series of PCN materials.

the inorganic nanolayers of the MMT clay in the organic PAA matrix via *in situ* UV photopolymerization. In this study, acrylamide monomers functioned as both the intercalating agent and reacting monomers. The as-synthesized PCN materials were characterized by FTIR spectroscopy, wide-angle powder X-ray diffraction, and TEM.

The effects of the material composition on the thermal stability, optical clarity, and gas-barrier properties of PAA and PCN materials, in the form of fine powders and membranes, were also studied by DSC, TGA, UV–vis transmission spectroscopy, and GPA. The molecular weights of PAA extracted from PCN materials and PAA were determined by GPC with THF as an eluant. The molecular weights of extracted PAA were significantly lower than that of bulk PAA, and this indicated the structurally restricted polymerization situations in the intragallery region of the MMT clay and the nature of the clay–oligomer interactions, such as adsorption, during the polymerization reaction. The thermal decomposition temperature and glass-transition temperature of the nanocomposites shifted significantly toward a temperature range higher than that of pristine PAA according to TGA and DSC studies, and this confirmed the enhancement of the thermal stability of the intercalated polymer. The optical

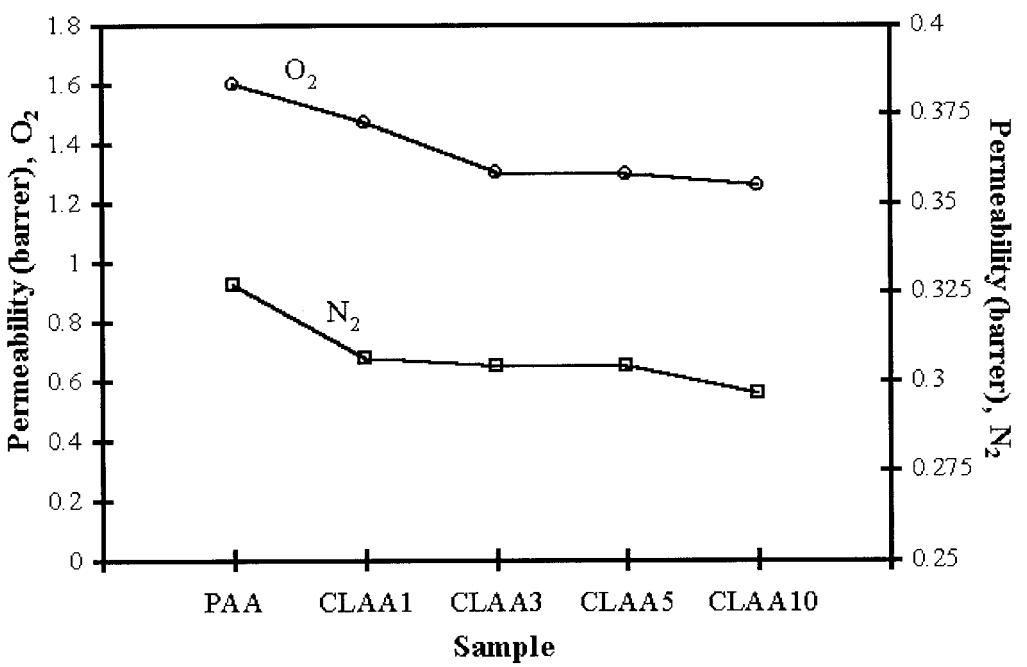

Figure 8 Permeability of O_2 and N_2 as a function of the MMT clay content in the PCN materials.

clarity of as-prepared PCN membranes remained high at low clay contents (e.g., CLAA1) according to a UV–vis transmission spectroscopy investigation, which yielded primarily exfoliated composites. The O_2 and N_2 molecular permeability properties of the PCN materials showed that the dispersion of clay platelets in PAA promoted the molecular barriers of the as-prepared membranes.

References

1. Yano, K.; Usuki, A.; Okada, A. J Polym Sci Part A: Polym Chem 1997, 35, 2289.
2. Wang, Z.; Pinnavaia, T. J. Chem Mater 1998, 10, 3769.
3. Lan, T.; Kaviratna, P. D.; Pinnavaia, T. J. Chem Mater 1994, 6, 573.
4. (a) Tyan, H.-L.; Liu, Y.-C.; Wei, K.-H. Chem Mater 1999, 11, 1942; (b) Yu, Y.-H.; Lin, C.-Y.; Yeh, J.-M.; Lin, W.-H. Polymer 2003, 44, 3553.
5. Gilman, J. W.; Jackson, C. L.; Morgan, A. B.; Hayyis, R., Jr.; Manias, E.; Giannelis, E. P.; Wuthenow, M.; Hilton, D.; Phillips, S. H. Chem Mater 2000, 12, 1866.
6. (a) Yeh, J.-M.; Liou, S.-J.; Lai, C.-Y.; Wu, P.-C.; Tsai, T.-Y. Chem Mater 2001, 13, 1131; (b) Yeh, J.-M.; Chen, C.-L.; Chen, Y.-C.; Ma, C.-Y.; Lee, K.-R.; Wei, Y.; Li, S. Polymer 2002, 43, 2729; (c) Yeh, J.-M.; Liou, S.-J.; Lin, C.-Y.; Cheng, C.-Y.; Chang, Y.-W.; Lee, K.-R. Chem Mater 2002, 14, 154; (d) Yeh, J.-M.; Chin, C.-P. J Appl Polym Sci 2003, 88, 1072; (e) Yeh, J.-M.; Chin, C.-P.; Chang, S. J Appl Polym Sci 2003, 88, 3264.
7. Gao, D.; Heimann, R. B.; Williams, M. C.; Wardhaugh, L. T.; Muhammad, M. J Mater Sci 1999, 34, 1543.
8. Churochkina, N. A.; Starodoubtsev, S. G.; Khokhlov, A. R. Polym Gels Networks 1998, 6, 205.
9. Meier, L. P.; Sheldon, R. A.; Caseri, W. R.; Suter, U. W. Macromolecules 1994, 27, 1637.
10. Wrobleski, D. A.; Benicewicz, B. C.; Thompson, K. G.; Byran, C. J. Polym Prepr (Am Chem Soc Div Polym Chem) 1994, 35(1), 265.
11. Xie, W.; Gao, Z.; Pan, W.-P.; Hunter, D.; Singh, A.; Vaia, R. Chem Mater 2001, 13, 2979.
12. Xie, W.; Xie, R.; Pan, W.-P.; Hunter, D.; Koene, B.; Tan, L. S.; Vaia, R. Chem Mater 2002, 14, 4837.
13. Wu, C.-G.; DeGroot, D. C.; Marcy, H. O.; Schindler, J. L.; Kannewurf, C. R.; Liu, Y.-J.; Hirpo, W.; Kanatzidis, M. G. Chem Mater 1996, 8, 1992.
14. Strawhecker, K. E.; Manias, E. Chem Mater 2000, 12, 2943.